AIP Applied Physics Letters

Dopant dependent band gap tailoring of hydrothermally prepared cubic Sr Ti x M 1 − x O 3 (M = Ru , Rh , Ir , Pt , Pd) nanoparticles as visible light photocatalysts

Sang Won Bae, Pramod H. Borse, and Jae Sung Lee

Citation: Applied Physics Letters **92**, 104107 (2008); doi: 10.1063/1.2897300

View online: http://dx.doi.org/10.1063/1.2897300

View Table of Contents: http://scitation.aip.org/content/aip/journal/apl/92/10?ver=pdfcov

Published by the AIP Publishing

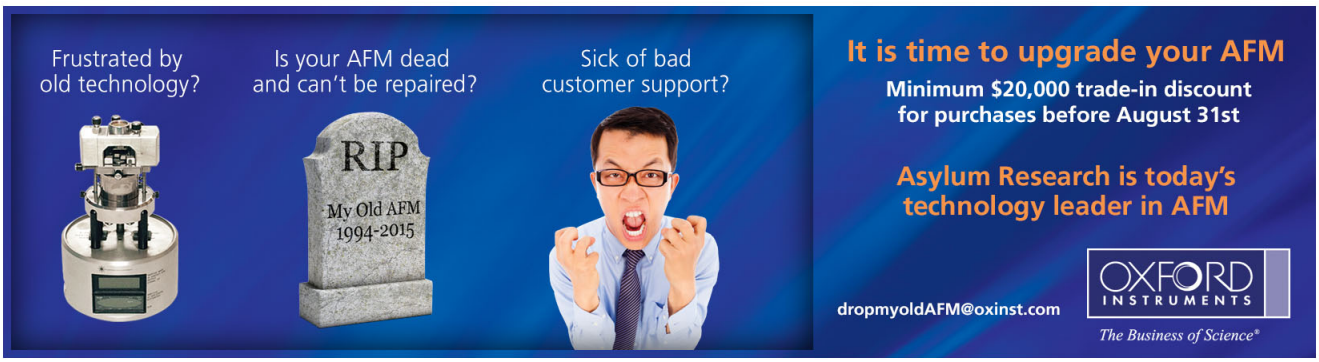

Dopant dependent band gap tailoring of hydrothermally prepared cubic $SrTi_xM_{1-x}O_3$ (M=Ru,Rh,Ir,Pt,Pd) nanoparticles as visible light photocatalysts

Sang Won Bae, Pramod H. Borse, and Jae Sung Lee[a)]
Eco-friendly Catalysis and Energy Laboratory (NRL), Department of Chemical Engineering, Pohang University of Science and Technology, Pohang 790-784, Republic of Korea

(Received 17 December 2007; accepted 16 February 2008; published online 14 March 2008)

Nanostructured cubic $SrTiO_3$ particles were hydrothermally synthesized and studied experimentally/theoretically for photoreduction of water. The particles were doped with metal atoms (M=Ru,Rh,Ir,Pt,Pd), which acquired high cyrstallinity after thermal treatment. $SrTiO_3$:Rh showed the highest rate of H_2 evolution under $\lambda > 420$ nm photons. The density functional theory calculations of $SrTi_xM_{1-x}O_3$ (M=Ru,Rh,Ir,Pt) implied that the photocatalytic activity of $SrTi_xRh_{1-x}O_3$ was due to its suitable band energetics, and the induced hybridized Ti/Rh orbitals in the bandgap of $SrTiO_3$. © *2008 American Institute of Physics*. [DOI: 10.1063/1.2897300]

Perovskite metal oxides have been demonstrated as efficient photocatalysts[1–3] for water splitting due to their suitable crystal lattice as well as possibly larger number of photocatalytic sites than the simple binary oxide photocatalysts (PCs). It is known that the introduction of a metal atom in the host lattice can tailor the electronic and physicochemical properties of the host lattice.[4,5] Thus, an UV PC can be converted to visible light (VL) PC desired in solar photocatalytic water splitting for hydrogen (H_2) energy generation. In present work, we study theoretically and experimentally the effect of doping noble metals (M=Ru,Rh,Ir,Pt,Pd) in the cubic lattice of $SrTiO_3$ (STO). We computed the electronic structure, synthesized experimentally the metal doped STO, and finally analyzed their photocatalytic activity of H_2 production from water using VL photons.

Chemical synthesis of nanostructured perovskite particles has been a challenging task[6,7] due to the high crystallization energy involved in the desired phase formation of the perovskite lattices. Especially STO, which crystallizes at very high temperatures ($T > 1273–1473$ K) (Ref. 8) offers difficulty in obtaining desired phase at lower temperatures. In the past,[8] the solid state reaction (SSR) method has been utilized for preparation of STO particles to yield randomly shaped particles with broadly dispersed sizes. Here, we use the hydrothermal (HT) method,[7] an economic and easy technique to synthesize the stable nanocubes at lower temperatures and improved their cyrstallinity by controlled thermal treatment to obtain single phase nanostructure STO. Then, we doped Ru, Rh, Ir, Pt, or Pd into STO using the HTs. Metal doping in a perovskite lattice at mild temperature conditions is a salient feature of the present work. We thus utilized prepared STO for solar H_2 generation.

$SrTiO_3$ and $SrTiO_3$:M (M=Ru,Rh,Ir,Pt,Pd) samples were synthesized by SSR and HT methods. In the SSR method, $SrCO_3$, and TiO_2 powders were mixed stoichiometrically in ethanol in an agate mortar, followed by vacuum drying (373 K) and calcination (1273 K/10 h). In HT method, the $Sr(OH)_2$, TiO_2, and C_2H_5OH were mixed in an agate mortar under N_2. The hydrothermal reaction was carried out in a Teflon-coated reactor (50 mL/pH > 13) at 443 K for 3 days. In syntheses of $SrTiO_3$:M (M=Ru,Rh,Ir,Pt,Pd), small amounts of metal precursors ($RuCl_3 \cdot nH_2O$, $RhCl_3 \cdot nH_2O$, $IrCl_3 \cdot nH_2O$, $H_2PtCl_6 \cdot nH_2O$, $PdCl_2$) were mixed before hydrothermal treatment. Thus, HT samples were washed, dried at 373 K, and calcined at 1073–1273 K.

The theoretical tool helps understanding of electronic properties of a photocatalytic system.[9] Thus, here, we correlated the theoretical and experimental results of STO:M (M=Ru,Rh,Ir,Pt,Pd). We used full potential linearized augmented plane wave method within density functional theory (WIEN97 package).[10] The atomic coordinates for STO were adopted from literature,[11] and a supercell with two STO units were employed for cubic $SrTi_{0.5}M_{0.5}O_3$ structures. We have also theoretically confirmed the feasibility of the formation of stable structures[12] of $SrTi_{0.5}M_{0.5}O_3$ (M=Ru,Rh,Ir,Pt,Pd) perovskite crystal structure for each system except for M=Pd.

Figure 1 shows the x-ray diffraction (XRD) patterns of undoped STO prepared by SSR and HT, and Rh-doped sample prepared by HT method followed by thermal treatment (1273 K/10 h), viz., calcined HT sample. All the

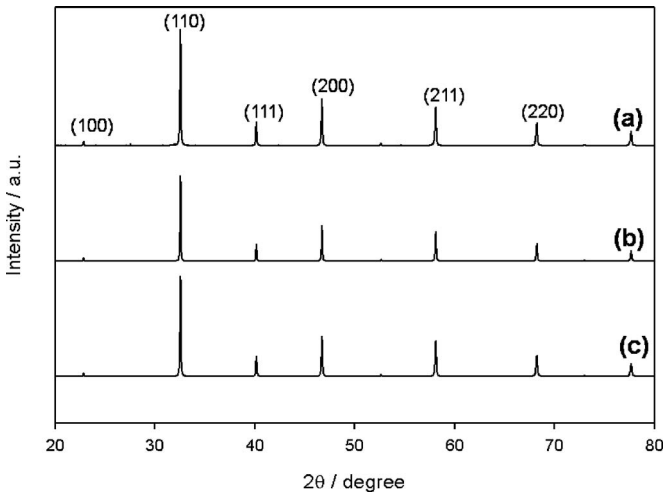

FIG. 1. X-ray diffraction patterns of $SrTiO_3$: (a) synthesized by SSR method, (b) synthesized by HT (uncalcined), and (c) $SrTiO_3$:Rh synthesized by HT and calcined at 1273 K for 10 h.

[a)]Author to whom correspondence should be addressed. Electronic mail: jlee@postech.ac.kr.

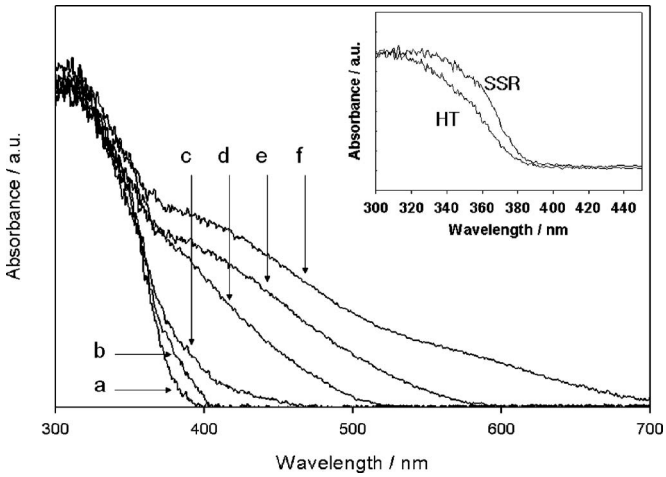

FIG. 2. UV-vis diffuse reflectance spectra for $SrTiO_3$ synthesized by SSR method (a); $SrTi_{0.99}M_{0.01}O_3$ (M=Pd,Pt,Rh,Ir,Ru), respectively [(b)–(f)], synthesized by HT and calcined at 1273 K for 10 h. The inset shows the spectra for pure $SrTiO_3$ synthesized by SSR and by HT (uncalcined).

samples exhibited the cubic phase of STO. As expected, the SSR sample showed highest cyrstallinity, although the calcined HT samples also displayed the similar cyrstallinity. There was no detectable impurity phase in any of the samples. The crystal lattice of the doped samples remains undisturbed even after doping, possibly due to the lower doping concentrations as confirmed by elemental analyses (energy dispersive spectroscopy and x-ray photoemission spectroscopy not shown). We selected 1 mol % M-doped samples, $SrTi_{0.99}M_{0.01}O_3$ (M=Ru,Rh,Ir,Pt,Pd) for further study, as they yielded the best photocatalytic activity in prescreening experiments. All doped samples exhibited the XRD patterns similar to the one shown in Fig. 1(c) for STO:Rh.

Figure 2 displays the UV-diffuse reflectance spectra of STO and $SrTi_{0.99}M_{0.01}O_3$ (M=Pd,Pt,Rh,Ir,Ru). The inset shows the UV-diffuse reflectance spectra (DRS) of uncalcined HT and SSR samples. The STO sample (SSR) showed a band edge absorption, whereas doped STO showed two absorption edges; the main edge due to the STO at 390 nm and a weak shoulder due to the doping of cation in the STO lattice. The dopant dependant absorption shows that $SrTi_{0.99}M_{0.01}O_3$ (M=Pt,Rh,Ir,Ru) can absorb more efficiently in visible range than pure STO and $SrTi_{0.99}Pd_{0.01}O_3$ sample. The difference in the absorption between HT and SSR samples mainly arises due to the existence of larger defect states in the HT sample. It is in direct agreement with crystallinity of the two systems as observed in Fig. 1. Upon calcination at 1273 K, the HT sample showed an absorption spectrum (not shown) similar to that of the SSR sample, which is also consistent with the improved crystallinity in Fig. 1. It is also important to note that the $SrTiO_3$:Pd sample appeared gray in color, and did not absorb VL, probably because in this case Pd metal might be loaded on the surface of the STO particle. All the other doped samples M=Pt,Rh,Ir,Ru, in order appeared gray, dark yellow, and red in color. This is consistent with estimated band gap energies of doped STO, i.e., Pd (3.1 eV), Pt (3.0 eV), Rh (2.5 eV), Ir (2.2 eV), and Ru (2.0 eV). It is already predicted that Pd-ionic radius is not suitable to dope in the STO lattice, and hence the result of optical absorption study in this case is not surprising. The optical absorption study clearly reveals that

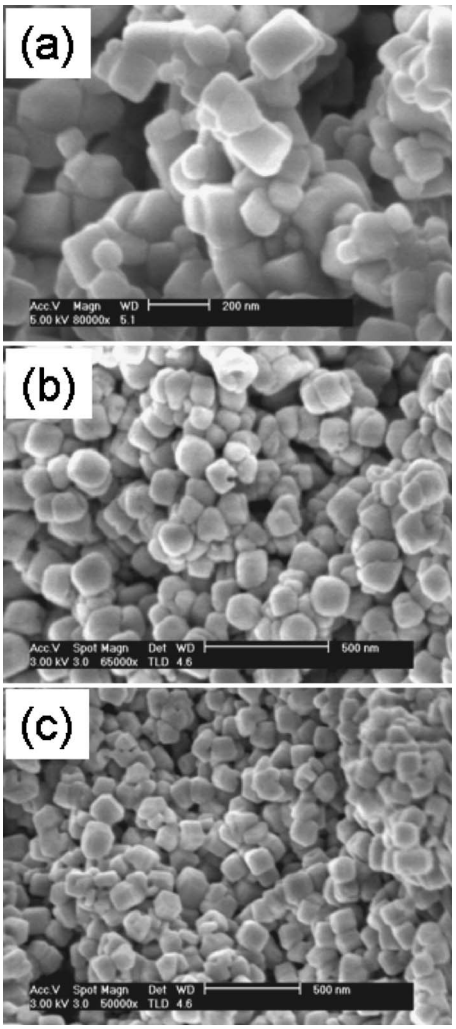

FIG. 3. SEM images of the particles of $SrTiO_3$, (a) synthesized by SSR, (b) synthesized by HT (uncalcined), and (c) $SrTiO_3$:Rh synthesized by HT and calcined at 1273 K for 10 h.

$SrTi_{0.99}M_{0.01}O_3$ (M=Rh,Ir,Ru) can more efficiently absorb the VL photons than others.

Figure 3 shows the field emission scanning electron microscopy (SEM) micrographs for pure STO (SSR and HT) and $SrTiO_3$:Rh (synthesized by HT and calcined). Interestingly stable cubic shaped nanoparticles are observed even after the high temperature (1273 K) calcination of particles prepared by HT method. The SSR sample displayed random shaped particles, whereas HT sample displayed cubic shape, which became better defined after calcination as seen in Fig. 3(c). In contrast to the particles size from SEM (100 nm in all case), Debye Scherrer analysis gave the estimate of 37 nm (Table I), which can be correlated to the average size of the constituent grains in the particles. Morphologies of the calcined HT samples of pure STO and $SrTi_{0.99}M_{0.01}O_3$ (M=Pd,Pt,Ir,Ru), were similar to Fig. 3(c), hence not displayed here. Thus, the formation of cubic STO nanoparticles is not affected by 1% doping.

Figure 4 shows the calculated densities of states (DOSs) for $SrTi_{0.5}M_{0.5}O_3$ (M=Ru,Rh,Ir,Pt) and STO. It is evident that the major contribution from metal orbital clearly tailors the band structure of the STO thereby yielding a reduction in the band gap (BG) as compared to the large BG of STO. The valence band width in each case of $SrTi_{0.5}M_{0.5}O_3$ (M

TABLE I. Crystal size, specific surface area and rate of H_2 evolution under UV irradiation from undoped $SrTiO_3$ photocatalyst.

Sample name	Crystal size (XRD) (nm)	BET area (g/m^2)	Activity[1] (μ mol H_2/h)
SSR	37.60	0.79	46
HT	34.46	7.20	40
HT 1073 K[2]	37.60	5.50	57
HT 1273 K[2]	37.60	3.42	67

[a]HT 1073 K; calcined at 1073 K for 10 h, HT 1273 K; calcined at 1273 K for 10 h.
[b]Photocatalytic reaction: Catalyst 0.1 g loaded with 1 wt% Pt; light source, 450 W, Hg-arc lamp (Oriel) in inner irradiation quartz cell. Reaction was performed in aqueous 10 mM NaOH solution (500 ml), pH > 11.

=Ru,Rh,Ir,Pt) was larger than STO. In addition, all the M-incorporated STO lattices displayed a strong hybridization of M orbital with the Ti 3d states of STO, thereby dominantly contributing to the top of the valence band and thus yielding a reduction in the BG of the host lattice. Such reduction in the BG is in clear agreement with optical absorption studies as described above, which is desirable for a VL active PC.

Further, we analyzed the photocatalytic properties of STO under UV radiation and for $SrTi_{0.5}M_{0.5}O_3$ (M =Ru,Rh,Ir,Pt) under VL radiation. The results of the photocatalytic H_2 evolution from aqueous solution (pH ~ 13) irradiated by UV are presented in Table I. Interestingly, cubic STO nanoparticles made by HT and calcination at 1273 K, showed much better H_2 evolution than STO synthesized by SSR method. The lower H_2 evolution from HT (uncalcined) is correlated to its lower crystallinity. Upon calcination at higher temperatures, larger amounts of H_2 were produced probably due to the increase in crystallinity. In all the cases stoichiometric amounts of oxygen were also evolved simultaneously. The complete analysis of the nanostructured STO indicates that their crystallinity dominantly affects/controls the photocatalytic activity, rather than their specific surface areas. The crystallinity was estimated by the intensity variation of (110) peak of STO in XRD (not shown here).

The dopant dependent VL photocatalytic H_2 evolution over nanostructured $SrTi_{0.99}M_{0.01}O_3$ (M=Ru,Rh,Ir,Pt,Pd) particles was measured for 0.2 g of catalyst under irradiation from 450 W, Hg-arc lamp with UV cutoff filter ($\lambda \geq 420$ nm) in an outer irradiation pyrex cell. Reaction was performed in aqueous methanol solution (methanol 10 ml+distilled water 90 ml). Only Rh, Ir, and Ru were photocatalytically active showing evolution rates of Rh (15.6 μmol/h) > Ir (1.1 μmol/h) > Ru (trace) > Pt (zero) ≈ Pd (zero). It is known[9] that a semiconductor PC would be active for water splitting provided its conduction (/valence) band edge is more negative (/positive) than the reduction (/oxidation) potential of water. Our theoretical study indicates that, treating STO as reference, only $SrTiO_3$:Rh shows the conduction band edge more negative than reduction potential of water thereby making it active for H_2 production. This observation correlates with the uniquely high activity for $SrTiO_3$:Rh. Further, Fig. 4 also indicates that the Ir/Ru states probably acts more as trapping centers that promote faster electron-hole recombination. As mentioned, 1 mol % Rh was the optimum concentration for producing efficient VL active $SrTiO_3$:Rh. The lower dopant concentrations seem to induce insufficient states to render VL absorption. In contrast, heavy Rh doping seems to provide a very high density of Rh induced states leading to recombination centers. The analysis suggests that VL photocatalytic activity in the nanostructured doped STO particles is interplay of the nature of dopant, dopant concentration, and high crystallinity of the nanoparticles.

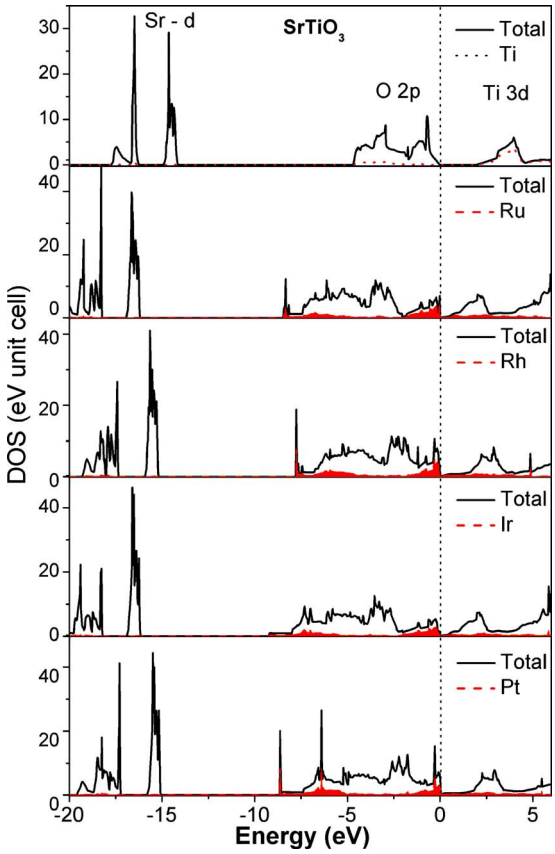

FIG. 4. (Color online) Total DOSs of cubic $SrTiO_3$ and $SrTi_{0.5}M_{0.5}O_3$ (M =Ru,Rh,Ir,Pt) calculated by FLAPW. Contributions of the dopant orbitals are shown by shaded area under the curves. Fermi level is adjusted to 0 eV. No stable structure was feasible for Pd.

This work was supported by Hydrogen Energy R&D Center of the Korean Ministry of Science and Technology and the Brain Korea 21 project.

[1]A. Kudo, Catal. Surv. Asia **7**, 31 (2003).
[2]H. G. Kim, P. H. Borse, W. Choi, and J. S. Lee, Angew. Chem., Int. Ed. **44**, 4585 (2005).
[3]H. G. Kim, D. W. Hwang, and J. S. Lee, J. Am. Chem. Soc. **126**, 8912 (2004).
[4]D. W. Hwang, H. G. Kim, J. S. Jang, S. W. Bae, S. M. Ji, and J. S. Lee, Catal. Today **93-95**, 845 (2004).
[5]T. Ishii, H. Kato, and A. Kudo, J. Photochem. Photobiol., A **163**, 181 (2004).
[6]P. H. Borse, U. A. Joshi, S. M. Ji, J. S. Jang, E. D. Jeong, H. G. Kim, and J. S. Lee, Appl. Phys. Lett. **90**, 034103 (2007).
[7]U. A. Joshi and J. S. Lee, Small **1**, 1172 (2005).
[8]R. Konta, T. Ishii, H. Kato, and A. Kudo, J. Phys. Chem. B **108**, 8992 (2004).
[9]P. H. Borse, J. S. Lee, and H. G. Kim, J. Appl. Phys. **100**, 124915 (2006).
[10]P. Blaha, K. Schwarz, and J. Luitz, WIEN97, Vienna University of Technology, Vienna, Austria, 1997 UNIX version WIEN code.
[11]S. A. Howard, J. K. Yau, and H. U. Anderson, J. Appl. Phys. **65**, 1492 (1989).
[12]M. W. Lufaso and P. M. Woodward, Acta Crystallogr., Sect. B: Struct. Sci. **57**, 725 (2001).